PRAMANA — journal of physics

Vol. 81, No. 4
October 2013
pp. 587–602

Elastic scattering and fusion cross-sections in ^{7}Li + ^{27}Al reaction

D PATEL[1,*], S SANTRA[2], S MUKHERJEE[1], B K NAYAK[2], P K RATH[1], V V PARKAR[2] and R K CHOUDHURY[2]

[1]Department of Physics, Faculty of Science, The M.S. University of Baroda, Vadodara 390 002, India
[2]Nuclear Physics Division, Bhabha Atomic Research Centre, Mumbai 400 085, India
*Corresponding author. E-mail: dipika.physics@gmail.com

MS received 29 January 2013; revised 14 June 2013; accepted 4 July 2013
DOI: 10.1007/s12043-013-0597-1; ***e*Publication:** 20 September 2013

Abstract. With an aim to understand the effects of breakup and transfer channels on elastic scattering and fusion cross-sections in the ^{7}Li + ^{27}Al reaction, simultaneous measurement of elastic scattering angular distributions and fusion cross-sections have been carried out at various energies ($E_{\rm lab}$ = 8.0–16.0 MeV) around the Coulomb barrier. Optical model (OM) analysis of the elastic scattering data does not show any threshold anomaly or breakup threshold anomaly behaviour in the energy dependence of the real and imaginary parts of the OM potential. Fusion cross-section at each bombarding energy is extracted from the measured α-particle evaporation energy spectra at backward angles by comparing with the statistical model prediction. Results on fusion cross-sections from the present measurements along with data from the literature have been compared with the coupled-channels predictions. Detailed coupled-channels calculations have been carried out to study the effect of coupling of breakup, inelastic and transfer, channels on elastic scattering and fusion. The effect of 1n-stripping transfer coupling was found to be significant compared to that of the projectile breakup couplings in the present system.

Keywords. Elastic scattering; fusion cross-sections; coupled-channels calculations; projectile breakup; continuum discretized coupled channels calculations; inelastic and transfer cross-sections.

PACS Nos 25.70.Bc; 25.70.Hi; 25.70.Jj; 24.10.Pa; 24.10.Eq

1. Introduction

The effect of breakup of weakly bound stable projectiles such as ^{6}Li, ^{7}Li, and ^{9}Be (with breakup threshold energies ranging from 1.47 to 2.47 MeV) on elastic scattering and fusion cross-sections is a subject of great interest, particularly at energies close to the Coulomb barrier [1–6]. The loss of flux from elastic channel goes to some of the reaction channels such as inelastic, breakup, transfer, and fusion, which changes the behaviour of the real and imaginary parts of the optical potential by showing 'threshold anomaly'

(TA) [5,7–9] and 'breakup threshold anomaly' (BTA) [10–12] in the reactions involving tightly and weakly bound nuclei. The above modification in effective (bare+polarization) potential for elastic channel at energies around the Coulomb barrier results in an enhancement or suppression in the corresponding fusion cross-sections.

There have been many measurements on elastic scattering involving stable weakly bound [13–23] as well as radioactive nuclei [24–26] with some contradictory observations. For example, it is reported that in the reaction of the weakly bound nuclei ^{7}Li + ^{138}Ba [18], and for ^{7}Li, ^{9}Be + ^{208}Pb [19,20], the so-called threshold anomaly (TA) is observed, but not in ^{9}Be + ^{209}Bi [21] reaction and also in the reanalysis of ^{7}Li + ^{138}Ba reaction [22]. Recently, experiments have been carried out for ^{6}Li + ^{112,116}Sn [10] and ^{6}Li + ^{209}Bi [11] systems, which have shown the existence of the so-called breakup threshold anomaly (BTA). In light mass systems ^{9}Be + ^{27}Al, ^{64}Zn [13,23], ^{6,7}Li + ^{28}Si [15,27], and ^{7}Li + ^{27}Al [28], the usual TA has not been observed. However, there is no clear understanding by which one can *a priori* predict the energy dependence of the optical model potentials around the Coulomb barrier.

On the other hand, for fusion measurements involving heavier targets, for instance ^{89}Y, ^{124}Sn, ^{144,152}Sm, ^{165}Ho, ^{206}Pb, ^{208}Pb, ^{209}Bi, with loosely bound projectiles, ^{6,7}Li, ^{9}Be, ^{6}He, fusion enhancement at the sub-barrier energies and suppression at above the Coulomb barrier energies have been reported [29–38]. For some of the medium mass targets, complete fusion cross-sections are not measured separately and it is mentioned that breakup does not affect the total fusion (complete fusion + incomplete fusion) at above-barrier energies [13,39,40]. A few measurements exist in the literature on fusion reactions with light mass targets at sub- and near-barrier energies. Ray *et al* [41] have carried out systematic comparisons of their fusion data on ^{6,7}Li + ^{24}Mg systems along with the data of ^{6,7}Li + ^{12,13}C [42–44], ^{16}O [45,46], ^{28}Si [47,48], ^{27}Al [49,50] systems. Most of these data are for above-barrier energies. For instance, Padron *et al* [49] have measured the total fusion cross-section for ^{7}Li system on ^{27}Al at well above the Coulomb barrier energy and have shown no evidence of suppression of the total fusion cross-section due to the breakup of the projectile as compared to the tightly bound nuclei. Kalita *et al* [50] have also obtained fusion excitation function for the same system at above-barrier energies which showed good agreement with the coupled-channels calculations using CCDEF code. It should be noted that for the ^{7}Li + ^{27}Al system, some preliminary data on fusion cross-section measurement are reported in a conference paper [51]. The results showed that the fusion cross-sections at sub- and near-barrier energies are on an average highly suppressed as compared to the ones involving other weakly bound projectiles such as ^{6}Li and ^{9}Be with the same target, although their measured data at above-barrier energies for the ^{7}Li + ^{27}Al system are in good agreement with the data reported in ref. [49]. Also, it is observed that the above data [51] at near- and sub-barrier energies are very much scattered. Thus, one cannot conclude about the enhancement or suppression of the fusion at this energy region. Therefore, it would be interesting to have new measurements on fusion cross-sections at energies around the Coulomb barrier for the ^{7}Li + ^{27}Al system. It will also be interesting to carry out a simultaneous measurement of elastic scattering and fusion cross-sections for the above system to address the effect of projectile (^{7}Li) breakup as well as nucleon transfer on these channels.

In view of the above motivations, measurements of both fusion cross-section and elastic scattering are carried out for the ^{7}Li + ^{27}Al system from below to above the Coulomb

barrier energies ($E_{\rm lab} \sim 8.0$ MeV $\leq V_{\rm b} \leq 16.0$ MeV). Though elastic scattering angular distribution for the present system exists in the literature (e.g., in ref. [28]), the α-evaporation energy spectra from which we propose to obtain fusion cross-section are not available. In order to avoid any systematic errors in the normalization of the α-energy spectrum to the elastic scattering at a particular angle and beam energy, it is of paramount importance that the data for the above channels are measured in the same experimental set-up. Detailed coupled-channels calculations are performed to study the effect of direct reaction channels on elastic scattering and fusion cross-sections with the potential and coupling parameters constrained by the data from the present measurements as well as the data from the literature.

The paper is organized as follows. The experimental details of the measurements are given in §2. In §3, optical model analysis of elastic scattering has been presented. Section 4 describes fusion cross-section measurements through α-particle evaporation spectra and their analysis. Further, in §5, the detailed coupled-channels calculations using FRESCO code are described. Finally, the results are summarized in §6.

2. Experimental details

The experimental measurements were performed with ^{7}Li beam using Folded Tandem Ion Accelerator (FOTIA) Facility at BARC, Mumbai, India. The elastic scattering and α-particle angular distribution measurements were carried out for the $^{7}\mathrm{Li} + {}^{27}\mathrm{Al}$ system ($V_{\rm b}^{\rm lab} \sim 8.3$ MeV) at six different bombarding energies 8, 9, 10, 12, 14, and 16 MeV. A self-supported ^{27}Al target having a thickness of $\sim$100 μg/cm^2 was used in the measurements, except for the measurement at 9 MeV beam energy where a target of $\sim$220 μg/cm^2 thickness was used. In data analysis, care has been taken to correct for energy loss of the beam in the target. Three telescopes ($\Delta E - E$) of silicon surface barrier detectors of thicknesses 22 μm + 1.5 mm, 17 μm + 1 mm and 15 μm + 300 μm respectively with a separation of 10° have been used. The solid angle subtended by each telescope was about 0.5 msr. Two Si surface barrier detectors of 300 μm thickness were kept at $\pm$20° with respect to the beam direction to measure Rutherford scattering for the purpose of normalization and to check the left–right beam wandering if any. The beam current was typically of the order of $\sim$10–15 nA. Measurements for elastic scattering angular distributions were performed in the angular range from 10° to 160°. For α-particle energy spectra (that were used to obtain fusion cross-section) measurements were carried out in the angular range of 110° to 150°.

A self-supported ^{12}C target of $\sim$50 μg/cm^2 thickness was used for α-particle energy calibration through $^{12}\mathrm{C}(^{7}\mathrm{Li},\alpha)^{15}\mathrm{N}$ reaction. The particle spectra measured by a telescope ($\Delta E - E$) showing discrete groups of α-particles with known energies produced in the above reaction were used for energy calibration as done by Parkar *et al* [52].

3. Optical model analysis of elastic scattering

The measured elastic scattering angular distribution data normalized to the Rutherford cross-sections (solid circles) as a function of the centre-of-mass angle ($\theta_{\rm c.m.}$) is shown in

figure 1. Optical model (OM) analysis of elastic scattering angular distributions data has been carried out using ECIS code [53]. Woods–Saxon (WS) form of potentials are used for both real and imaginary parts of the OM potential. In the OM analysis, the real (V) and imaginary (W) potential depths have been varied to get the best fit to the experimental data with minimum χ^2 value. The reduced radius (r_0) and diffuseness (a_r and a_i) parameters have been kept constant at 1.2 fm and 0.63 fm respectively. The OM fit at all energies are shown by continuous lines in figure 1. In order to avoid ambiguities with many sets of potential parameters, a radius of sensitivity (R_s), where different sets of potential parameters give equal potential value, has been obtained by the method described in [10]. From the derived value of the radius of sensitivity R_s (∼8.0 fm) and mean value of diffuseness parameters a_r and a_i (0.63 fm), the energy dependence of both the real and imaginary potentials are shown in figure 2. Potential parameters along with total reaction cross-sections obtained from OM fit at each energy are given in table 1. It is observed that the energy dependence of the real and imaginary parts of the OM potential obtained from the present elastic scattering angular distribution data does not show any particular trend of either TA or BTA unlike those observed in refs [10–12], but consistent with the observation made by Figueira *et al* [28] for the same system.

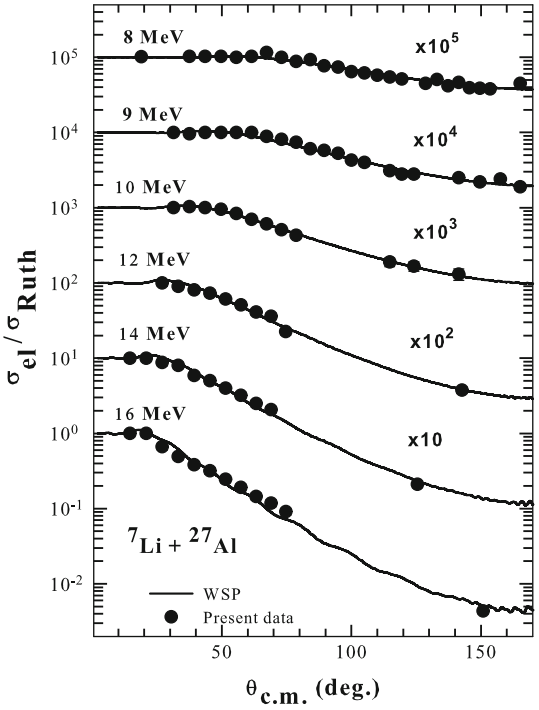

Figure 1. Measured elastic scattering angular distributions normalized to the Rutherford cross-sections (filled circles) as a function of $\theta_{c.m.}$ for the ^{7}Li + ^{27}Al system. Solid lines represent the OM fit to the data using Woods–Saxon potentials in ECIS code [53].

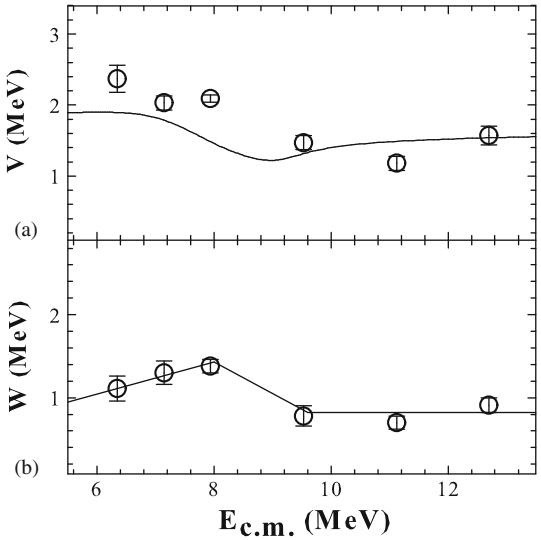

Figure 2. Bombarding energy ($E_{\text{c.m.}}$) dependence of the value of (**a**) real and (**b**) imaginary parts of Woods–Saxon potential at R_s (∼8.0 fm) for the $^{7}\text{Li} + {}^{27}\text{Al}$ system. Solid lines correspond to dispersion relation calculation.

Table 1. WS potential parameters and total reaction cross-sections obtained from the OM analysis of the elastic scattering data for the $^{7}\text{Li} + {}^{27}\text{Al}$ system. The radius and diffuseness parameters are chosen to be constant at $R_r = R_i = 5.90$ fm, where $R_r = R_i = r_0(A_p^{1/3} + A_t^{1/3})$ and $a_r = a_i = 0.63$ fm.

E_{lab} (MeV)	$E_{\text{c.m.}}$ (MeV)	V (MeV)	W (MeV)	χ^2_{min}/N	σ_{reac} (mb)
8.0	6.35	61.25	28.61	1.71	289
9.0	7.15	52.54	33.57	1.82	487
10.0	7.94	54.14	35.58	0.45	682
12.0	9.53	37.92	20.09	0.76	869
14.0	11.12	30.57	18.18	0.89	1015
16.0	12.7	40.62	23.61	2.75	1224

The consistency of the present results on real and imaginary parts (V and W) of the complex optical potential $U(r, E) = -V(r, E) - iW(r, E)$ has been tested by the dispersion relation analysis [54]. The energy dependence of the real potential (V) is obtained by the above dispersion relation calculations by assuming the energy-dependent imaginary potential to be made of three straight line segments (as shown in figure 2b). It is observed that the trend of the energy dependence of the real potential is reproduced (as shown by a solid line in figure 2a). Hence, both the real and the imaginary parts of the OM potential are consistent.

4. Fusion cross-section from measured α-spectra

Fusion cross-sections have been extracted at five different bombarding energies corresponding to 8, 9, 10, 14, and 16 MeV from the α-particle energy spectra measured at backward angles. The measured α-particle spectra can have contributions from both compound nuclear formation and direct reaction channels such as breakup and/or transfer. To estimate the contributions from direct reactions, coupled-channels calculations using FRESCO (as described in §5) is performed. The α contributions can arise from the projectile breakup ($^7\mathrm{Li} \rightarrow \alpha + t$) or transfer followed by breakup channels. The breakup contribution has been obtained from the CDCC calculations. It is found that, at backward angles, the contributions from the projectile breakup to measured α-particles are negligible. One of the important transfer channels that can contribute to alpha yield is

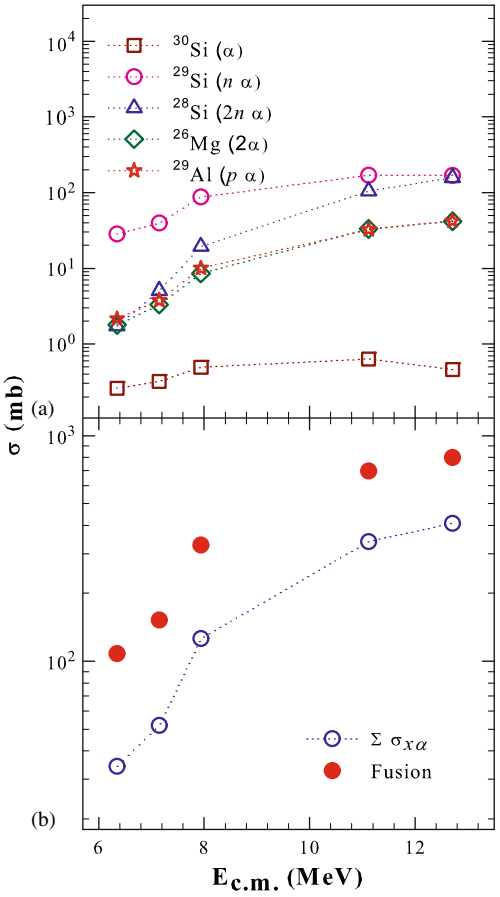

Figure 3. (**a**) Cross-sections for different α-particle evaporation channels in $^7\mathrm{Li} + ^{27}\mathrm{Al}$ reaction from the predictions of PACE code. (**b**) Comparison of cross-sections for the sum of different α-particle evaporation channels and total fusion in $^7\mathrm{Li} + ^{27}\mathrm{Al}$ reaction.

the $1p$-pickup by ^{7}Li to form ^{8}Be, which in turn can break into two α-particles. In ^{7}Li + ^{209}Bi reaction [55] it was observed that this channel has a substantial contribution towards alpha production. However, from the coupled-channels calculations, it is observed that the cross-sections for the $1p$-pickup channel at backward angles are much smaller compared to the evaporation alpha yields. Also, for a similar light mass system ^{7}Li + ^{28}Si [47], it is verified that the contributions to α-particle spectra are mostly from the compound reaction channels at backward angles. From the PACE [56] calculations, the different possible α-particle evaporation channels are shown in figure 3a. It is found that the combined cross-sections of the above α-particle evaporation channels constitute ~32–50% of the total fusion cross-sections over the measured energy range as demonstrated in figure 3b.

The measured evaporated α-particle energy spectra were compared to the results of Monte Carlo statistical model code PACE [56] to obtain the fusion cross-section as done in ref. [52]. The α-particle evaporation spectra were obtained in energy bins of 1.0 MeV width. The $\mathrm{d}\sigma_\alpha/\mathrm{d}\Omega$ is extracted using the relation given below:

$$\frac{\mathrm{d}\sigma_\alpha}{\mathrm{d}\Omega} = \frac{\mathrm{d}\sigma_{\mathrm{el}}}{\mathrm{d}\Omega} \times \frac{Y_\alpha}{Y_{\mathrm{el}}}, \tag{1}$$

where $\mathrm{d}\sigma_\alpha/\mathrm{d}\Omega$, Y_α and $\mathrm{d}\sigma_{\mathrm{el}}/\mathrm{d}\Omega$, Y_{el} are the differential cross-sections and yields of α-particle emission and elastic scattering respectively.

The magnitude of total fusion cross-section in the PACE input is optimized to get the best fit with the experimental α-evaporation spectra. In the PACE code, the spin distribution following the fusion was parametrized as a Fermi distribution:

$$\sigma_l = \frac{(\pi/k^2)(2l+1)}{1+\exp((l-l_{\max})/\Delta)}, \tag{2}$$

where Δ is the diffuseness parameter, k is the wave number, and the variable $l_{\max}$ was determined from the relation, $\sigma_{\mathrm{fus}} = \sum_{l=0}^{l_{\max}} \sigma_l$. The level density parameter was set at $A/10$. This method worked well for comparing and optimizing the α-particle energy spectra predicted by PACE [56] with the ones from the measurement. Thus, the experimental fusion cross-sections were obtained. The fusion cross-sections obtained at different energies are listed in table 2. Figure 4 shows a comparison between measured and PACE-predicted α-particle energy spectra at different angles and bombarding energies. In figure 5 the fusion cross-sections (σ_{fus}) obtained from the present measurements are plotted as a function of energy ($E_{\mathrm{c.m.}}$) along with the available data in the literature. It can be observed that the

Table 2. Fusion cross-sections for the ^{7}Li + ^{27}Al system at various bombarding energies extracted from the measured α-particle spectra.

E_{lab} (MeV)	$E_{\mathrm{c.m.}}$ (MeV)	σ_{fus} (mb)
8.0	6.35	108±14
9.0	7.15	152±20
10.0	7.94	327±40
14.0	11.12	697±87
16.0	12.7	800±100

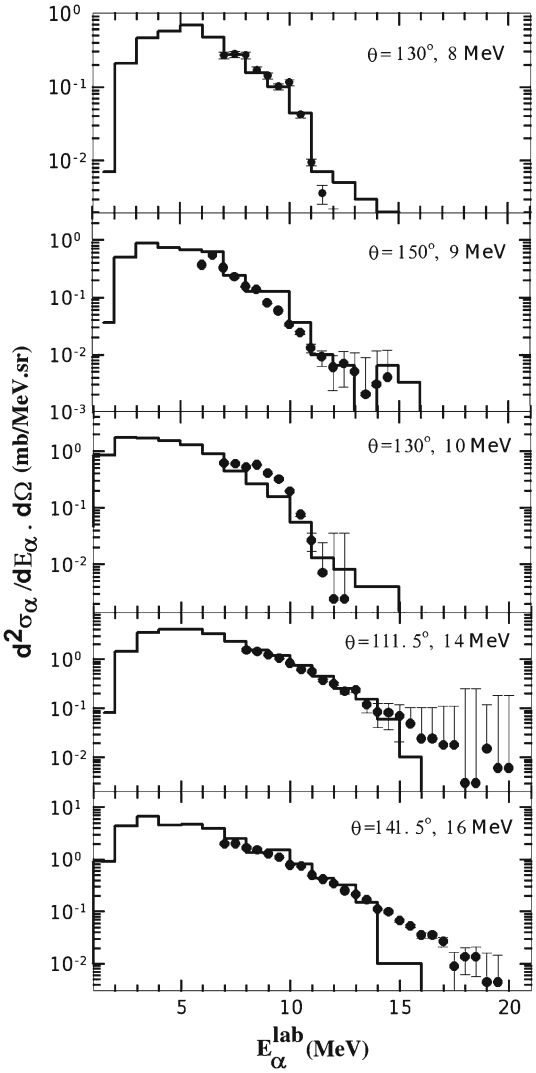

Figure 4. The α-particle energy spectra measured at various energies in ^{7}Li + ^{27}Al reaction along with the predictions of PACE code. The filled circles show experimental data points and PACE calculations are shown by histograms. All the angles and energies are represented in laboratory system.

present fusion cross-sections at the above-barrier energies match well with the available literature data [49,50] and at sub-barrier energies they are systematically increasing with the energy. The solid curve in figure 5 shows the predictions of CCFULL code [57], for fusion excitation function with inelastic coupling to target excited state. No-coupling calculations are not plotted in the figure as they show no difference with calculations including inelastic coupling. The coupling of the target inelastic state at 0.842 MeV with

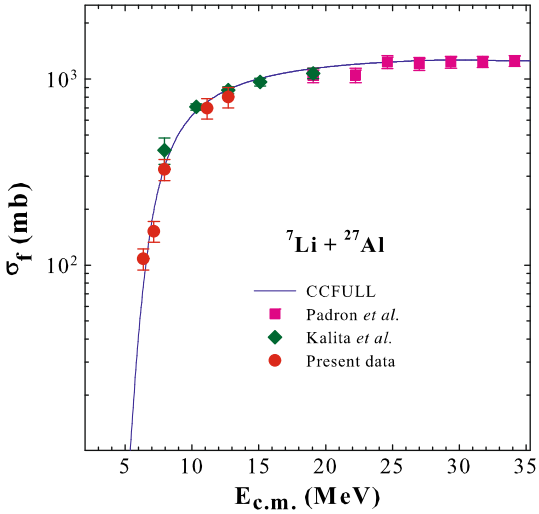

Figure 5. Comparison of fusion cross-sections obtained in the present experiment with data from the literature and CCFULL predictions for the ^{7}Li + ^{27}Al system. Filled circles represent fusion cross-sections from the present measurement. Filled squares and diamonds represent the fusion data from refs [49] and [50] respectively. CCFULL calculated fusion cross-sections are represented by a solid line.

deformation parameter $\beta_2 = 0.31$ has been considered in the calculations. The barrier parameters used in the CCFULL calculation are: $V_b = 6.6$ MeV, $R_b = 7.97$ fm and $\hbar\omega = 3.39$ MeV, providing a reasonable agreement with the present experimental data at near-barrier energies as well as the fusion data available in literature at above-barrier

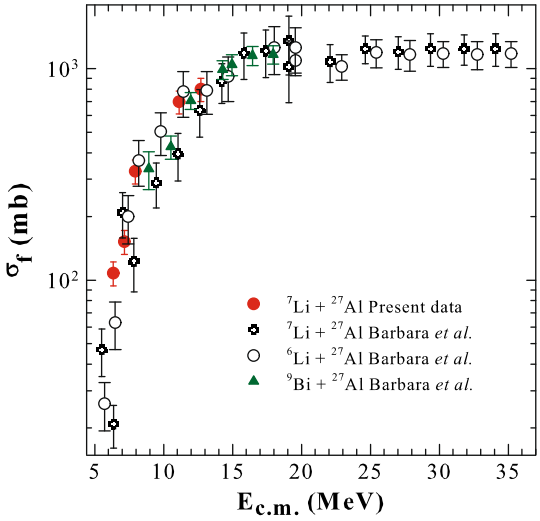

Figure 6. Comparison of fusion cross-sections in the reactions of ^{6,7}Li and ^{9}Be with ^{27}Al target at around the Coulomb barrier energies.

energies. The barrier height used for the above calculations is consistent with the barrier height mentioned in ref. [58]. It can be observed that the effect of target inelastic coupling is insignificant (similar to the observation made by Kalita *et al* [50]) due to the low Z value of the target.

In addition, we have compared the fusion cross-sections in reactions of different weakly bound projectiles ^{6,7}Li, ^{9}Be with ^{27}Al target as shown in figure 6. The data have been included from the present work and ref. [51]. It is observed that the present fusion data for ^{7}Li + ^{27}Al reaction at energies around the Coulomb barrier are of the same order as that of ^{6}Li + ^{27}Al [51].

5. Coupled-channels calculations

In order to unfold the effect of couplings of direct reaction channels such as breakup, inelastic and transfer on elastic and fusion cross-sections, the continuum discretized coupled channels (CDCC) and coupled reaction channels calculations (CRC) have been carried out using FRESCO code [59], version FRES 2.8. In the CDCC calculations, the structure of the projectile ^{7}Li has been considered as a cluster of α (core) and t (valence). The continuum of ^{7}Li ($\alpha + t$) up to the excitation energy of 5 MeV has been considered. It includes the first resonant state ($7/2^-$, 4.63 MeV) with a width of 0.093 MeV. The non-resonant continuum has been discretized in terms of momentum bins of finite width, $\Delta k = 0.20$ fm^{-1}, and the region around the resonant state has been discretized into much smaller momentum bins ($\Delta k \sim 0.0050$ fm^{-1}). The scattering states arising from the combinations of α and t have been assumed as excited states of ^{7}Li with the energy equal to the mean of bin energy range. The scattering wave functions in the solution of coupled-channels calculations have been integrated up to 80 fm in steps of 0.02 fm and the relative angular momentum up to $95\hbar$ has been considered.

In addition to the projectile breakup, some of the important direct reaction channels are also included. In the final coupled-channels calculations, the couplings that are included to study their effects on elastic scattering and fusion reactions are: projectile breakup channels, bound excited state ($1/2^-$, 478 keV state) of ^{7}Li, and $1n$-stripping transfer channels. The experimental data on elastic, inelastic, and transfer channels act as constraints to the potential and coupling parameters that are used in the FRESCO calculations.

The coupling potentials for $\alpha + ^{27}$Al and $t + ^{27}$Al have been taken from refs [60,61] to obtain the cluster-folded (CF) potential for the entrance channel. The strength of the real part of the CF potential was needed to be multiplied by a factor of 0.6 to reproduce the measured elastic scattering cross-sections at all energies.

The results for the elastic scattering from the above coupled-channels calculations are compared with the present experimental data as well as the ones from [28] as shown in figure 7. It is observed that the calculations reproduce the elastic scattering data reasonably well over the entire energy range of our measurement. The calculations with no coupling, only breakup coupling and breakup+transfer couplings are represented by dotted, dashed, and solid lines respectively. It is interesting to note that the effect of transfer coupling on elastic scattering particularly at above-barrier energies is significant and more than that of breakup couplings. This can be understood in terms of the reaction probabilities of these two channels as demonstrated in figure 8, where the calculated breakup

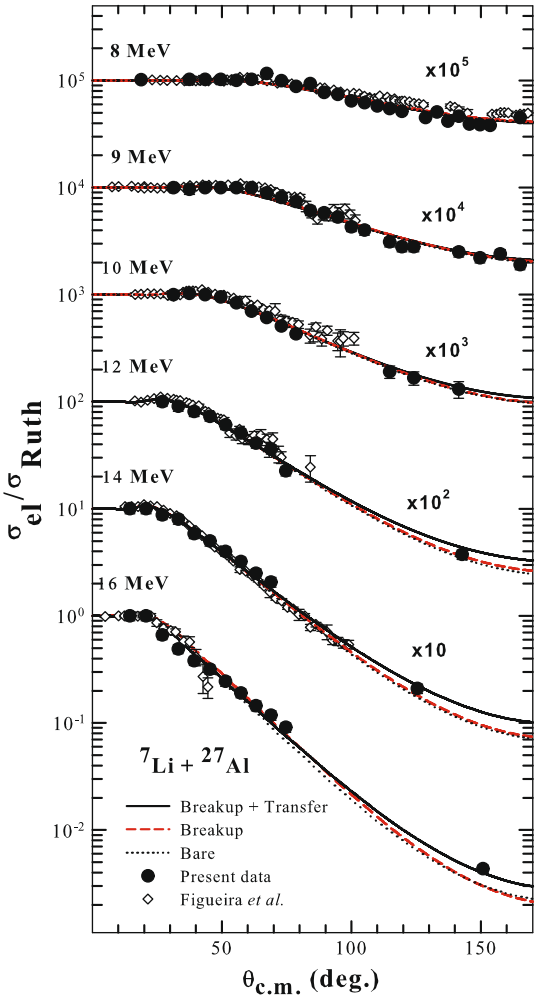

Figure 7. Elastic scattering cross-sections normalized to the Rutherford cross-sections as a function of $\theta_{\text{c.m.}}$ for the scattering of ^{7}Li from ^{27}Al. The filled circles show the present experimental data points. The open diamonds represent data points from ref. [28]. The dotted, dashed (red), and solid (black) lines represent the calculations with no coupling, breakup, and full (breakup+transfer) couplings respectively.

and transfer cross-sections are compared as a function of energy. It clearly shows the dominance of transfer over breakup at all the energies.

Coupling to the inelastic scattering corresponding to the projectile (^{7}Li) bound excited state ($1/2^{-}$, 478 keV) has been included in the above CDCC calculations. Coupling of this state is taken similar to the one of the discrete continuum states. The calculated inelastic cross-sections (solid lines) are compared with the experimental data (filled circles) available in [62] at three energies ($E_{\text{lab}} = 11$ MeV, 14 MeV, and 18 MeV) as shown in

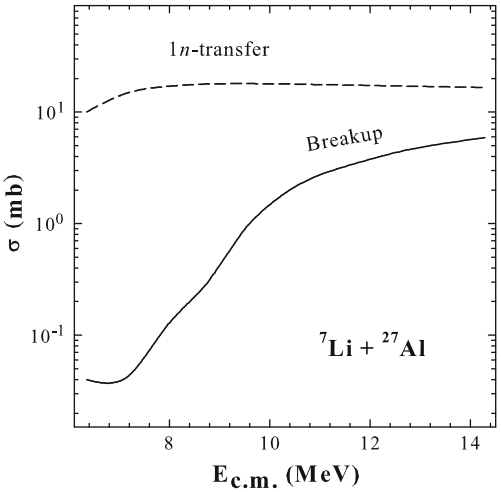

Figure 8. Calculated breakup and transfer cross-sections from the coupled-channels calculations using FRESCO, as a function of $E_{\text{c.m.}}$ in the reaction of ^{7}Li + ^{27}Al.

figure 9. The results are shown as solid lines which are reasonably close to the experimental data.

To study the effect of transfer channels, the dominant $1n$-stripping channel, i.e., ^{27}Al(^{7}Li,^{6}Li)^{28}Al was included along with the CDCC calculations. The ground state (3^+) and 0.031 MeV (2^+) states of ^{28}Al have been included in the calculations. The spectroscopic factors were taken from refs [62,63]. The results of the neutron transfer calculations are compared with the experimental data available in [62] at three different

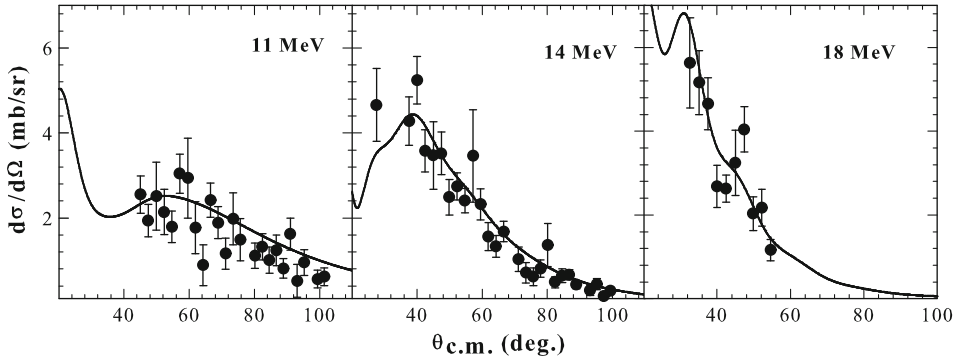

Figure 9. Comparison of experimental data and calculations for inelastic cross-sections, as a function of $\theta_{\text{c.m.}}$ at 11, 14 and 18 MeV beam energies in the ^{7}Li + ^{27}Al reaction. The filled circles represent the experimental data for inelastic cross-sections [62]. The solid line shows the calculated inelastic cross-sections corresponding to the bound excited state ($1/2^-$, 478 keV) of ^{7}Li.

energies. It can be observed that the calculations are in good agreement with the measured experimental data of transfer cross-sections corresponding to the g.s. plus 2^+ state of ^{28}Al as shown in figure 10.

Further, an attempt has been made to understand the experimental fusion data and the reaction cross-sections derived from the OM analysis of the elastic scattering data in terms

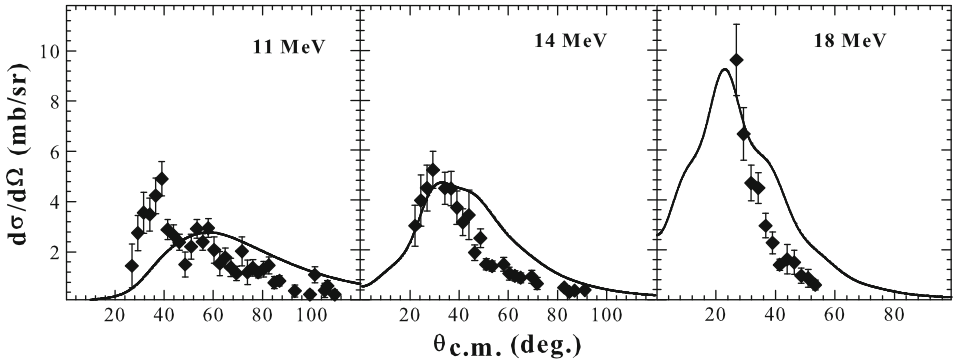

Figure 10. Comparison of experimental data and calculations for transfer cross-sections at 11, 14 and 18 MeV. The filled diamonds correspond to the experimental data on transfer cross-sections [62]. The solid line represents the sum of the $1n$-transfer cross-sections corresponding to the g.s. plus 2^+ state of ^{28}Al.

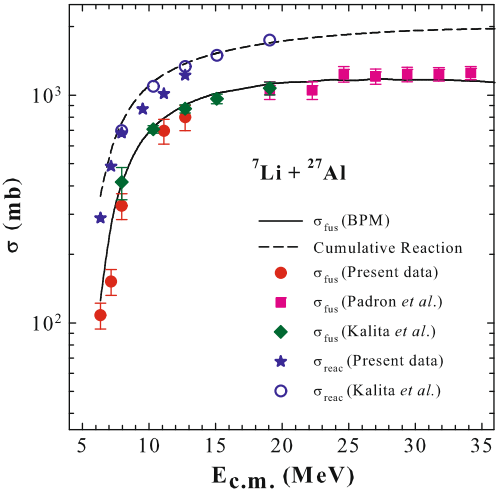

Figure 11. Comparison of fusion cross-sections obtained from the coupled-channels calculations for the ^{7}Li + ^{27}Al reaction with the present measurement (filled circles) and the data from the literature [49] (filled squares). The solid and dashed lines represent the BPM fusion and cumulative reaction cross-sections respectively obtained from the CDCC calculations with breakup+transfer couplings using FRESCO.

of CDCC+transfer calculations using FRESCO. Fusion cross-section was obtained by the barrier penetration model (BPM) option of FRESCO and shown in figure 11 as a solid line. It can be observed that both the reaction cross-sections (dashed line) and fusion cross-sections (solid line) calculated from FRESCO are very close to the experimental data.

6. Summary and conclusions

Elastic scattering and fusion cross-section measurements have been carried out in ^{7}Li + ^{27}Al reaction at near-barrier energies. Optical model analysis employing Woods–Saxon form of potentials has been performed to extract the OM potential parameters. No strong conclusion regarding the presence of the TA or the BTA could be made on the basis of the energy dependence of the OM potentials, consistent with earlier results in the literature. The elastic scattering angular distributions have also been analysed by means of CDCC and transfer calculations using FRESCO. Couplings to the bound inelastic state of the projectile has also been included. The present elastic scattering angular distributions are nicely explained by the CDCC+inelastic+1n-transfer calculations. These calculations are performed using the potential and coupling parameters that are constrained by the experimental data for elastic, inelastic (first excited state of ^{7}Li), and 1n-stripping transfer (corresponding to the g.s. plus 2^{+} state of ^{28}Al) channels available from this work and from the literature. The effect of 1n-transfer coupling on elastic scattering was found to be more important as compared to breakup couplings particularly at above-barrier energies.

Fusion cross-sections at energies near the Coulomb barrier were obtained from the measured α evaporation spectra at backward angles. Present data along with the literature data by Padron *et al* [49] in the above-barrier energies are well represented by the predictions of the simplified coupled-channels fusion model (CCFULL) calculations assuming a fusion barrier height of 6.6 MeV (consistent with ref. [58]). A comparison of fusion cross-section involving the same target (^{27}Al) and three weakly bound stable projectiles (^{6,7}Li, ^{9}Be) shows that the present fusion data involving ^{7}Li is similar to those involving ^{6}Li [51] around the Coulomb barrier energies, and do not show any suppression compared to the other two reactions (^{6}Li, ^{9}Be + ^{27}Al), which is contrary to the observation in ref. [51]. Fusion cross-sections were also calculated by CDCC+transfer calculations using FRESCO. Fusion by BPM calculation was found to agree with the experimental data reasonably well.

Acknowledgements

The authors would like to thank FOTIA staff at BARC for their cooperation during the experiment and Dr S Kailas for fruitful discussions. D Patel and S Mukherjee gratefully acknowledge the financial support from DAE-BRNS (No. 2008/37/42) through a major research project. V V Parkar acknowledges the financial support of INSPIRE Faculty Award, Department of Science and Technology, Govt. of India for carrying out these investigations.

References

[1] Y Tokimoto *et al*, *Phys. Rev. C* **63**, 035801 (2001)
[2] N Keeley *et al*, *Prog. Part. Nucl. Phys.* **59**, 579 (2007)
[3] E A Benjamim *et al*, *Phys. Lett. B* **647**, 30 (2007)
[4] L F Canto, P R S Gomes, R Donangelo and M S Hussein, *Phys. Rep.* **424**, 1 (2006)
[5] G R Satchler, *Phys. Rep.* **199**, 147 (1991)
[6] D Patel *et al*, *AIP Conf. Proc.* **1524**, 171 (2013)
[7] M A Nagarajan, C C Mahaux and G R Satchler, *Phys. Rev. Lett.* **54**, 1136 (1985)
[8] S Santra *et al*, *Phys. Rev. C* **60**, 034611 (1999)
[9] M E Brandan and G R Satchler, *Phys. Rep.* **285**, 143 (1997)
[10] N N Deshmukh *et al*, *Phys. Rev. C* **83**, 024607 (2011)
[11] S Santra, S Kailas, K Ramachandran, V V Parkar, V Jha, B J Roy and P Shukla, *Phys. Rev. C* **83**, 034616 (2011)
[12] L Fimiani *et al*, *Phys. Rev. C* **86**, 044607 (2012)
[13] S B Moraes *et al*, *Phys. Rev. C* **61**, 064608 (2000)
[14] S Mukherjee *et al*, *Eur. Phys. J. A* **45**, 23 (2010)
[15] A Pakou *et al*, *Phys. Lett. B* **556**, 21 (2003)
[16] J M Figueira *et al*, *Phys. Rev. C* **81**, 024613 (2010)
[17] N N Deshmukh *et al*, *Eur. Phys. J. A* **47**, 118 (2011)
[18] A M M Maciel *et al*, *Phys. Rev. C* **59**, 2103 (1999)
[19] R J Woolliscroft, B R Fulton, R L Cowin, M Dasgupta, D J Hinde, C R Morton and A C Berriman, *Phys. Rev. C* **69**, 044612 (2004)
[20] N Keeley, S J Bennett, N M Clarke, B R Fulton, G Tungate, P V Drumm, M A Nagarajan and J S Lilley, *Nucl. Phys. A* **571**, 326 (1994)
[21] C Signorini *et al*, *Phys. Rev. C* **61**, 061603 (2000)
[22] P R S Gomes *et al*, *J. Phys. G* **31**, S1669 (2005)
[23] P R S Gomes *et al*, *Phys. Rev. C* **70**, 054605 (2004)
[24] E F Aguilera *et al*, *Phys. Rev. C* **79**, 021601 (2009)
[25] A R Garcia, J Lubian, I Padron, P R S Gomes, T Lacerda, V N Garcia, A Gomez Camacho and E F Aguilera, *Phys. Rev. C* **76**, 067603 (2007)
[26] K Rusek, *Eur. Phys. J. A* **41**, 399 (2009)
[27] A Pakou *et al*, *Phys. Rev. C* **69**, 054602 (2004)
[28] J M Figueira *et al*, *Phys. Rev. C* **73**, 054603 (2006)
[29] M Dasgupta *et al*, *Phys. Rev. L* **82**, 1395 (1999)
[30] V V Parkar *et al*, *Phys. Rev. C* **82**, 054601 (2010)
[31] P K Rath *et al*, *Phys. Rev. C* **79**, 051601R (2009)
[32] P K Rath *et al*, *Nucl. Phys. A* **874**, 14 (2012)
[33] C S Palshetkar *et al*, *Phys. Rev. C* **82**, 044608 (2010)
[34] V Jha and S Kailas, *Phys. Rev. C* **80**, 034607 (2009)
[35] Y W Wu, Z H Liu, C J Lin, H Q Zhang, M Ruan, F Yang, Z C Li, M Trotta and K Hagino, *Phys. Rev. C* **68**, 044605 (2003)
[36] V Tripathi, A Navin, K Mahata, K Ramachandran, A Chatterjee and S Kailas, *Phys. Rev. Lett.* **88**, 172701 (2002)
[37] Yu E Penionzhkevich, V I Zagrebaev, S M Lukyanov and R Kalpakchieva, *Phys. Rev. Lett.* **96**, 162701 (2006)
[38] M Dasgupta *et al*, *Phys. Rev. C* **66**, 041602(R) (2002)
[39] R M Anjos *et al*, *Phys. Lett. B* **534**, 45 (2002)
[40] P R S Gomes *et al*, *Phys. Lett. B* **601**, 20 (2004)
[41] M Ray *et al*, *Phys. Rev. C* **78**, 064617 (2008)

[42] L C Dennis, K M Abdo, A D Frawley and K W Kemper, *Phys. Rev. C* **26**, 981 (1982)
[43] A Mukherjee, U Datta Pramanik, S Chattopadhyay, M Saha Sarkar, A Goswami, P Basu, S Bhattacharya, M L Chatterjee and B Dasmahapatra, *Nucl. Phys. A* **635**, 305 (1998)
[44] A Mukherjee, U Datta Pramanik, M Saha Sarkar, A Goswami, P Basu, S Bhattacharya, S Sen, M L Chatterjee and B Dasmahapatra, *Nucl. Phys. A* **596**, 299 (1996)
[45] J F Mateja, J Garman, D E Fields, R L Kozub, A D Frawley and L C Dennis, *Phys. Rev. C* **30**, 134 (1984)
[46] A Mukherjee, U Datta Pramanik, S Chattopadhyay, M Saha Sarkar, A Goswami, P Basu, S Bhattacharya, M L Chatterjee and B Dasmahapatra, *Nucl. Phys. A* **645**, 13 (1999)
[47] Mandira Sinha *et al*, *Phys. Rev. C* **76**, 027603 (2007)
[48] M Hugi *et al*, *Nucl. Phys. A* **368**, 173 (1981)
[49] I Padron *et al*, *Phys. Rev. C* **66**, 044608 (2002)
[50] K Kalita *et al*, *Phys. Rev. C* **73**, 024609 (2006)
[51] E de Barbara *et al*, *AIP Conf. Proc.* **884**, 189 (2007), DOI: 10.1063/1.2710578
[52] V V Parkar, K Mahata, S Santra, S Kailas, A Shrivastava, K Ramachandran, A Chatterjee, V Jha and P Singh, *Nucl. Phys. A* **792**, 187 (2007)
[53] J Raynal, *Phys. Rev. C* **23**, 2571 (1981)
[54] C Mahaux, H Ngo and G R Satchler, *Nucl. Phys. A* **449**, 354 (1986)
[55] D H Luong, M Dasgupta, D J Hinde, R du Rietz, R Rafiei, C J Lin, M Evers and A Diaz-Torres, *Phys. Lett. B* **695**, 105 (2011)
[56] A Gavron, *Phys. Rev. C* **21**, 230 (1980)
[57] K Hagino, N Rowley and A T Kruppa, *Comput. Phys. Commun.* **123**, 143 (1999)
[58] D Abriola *et al*, *Nucl. Instrum. Methods Phys. Res. B* **268**, 1793 (2010)
[59] I J Thompson, *Comput. Phys. Rep.* **7**, 167 (1988)
[60] K W Kemper, A W Qbst and R L Whit, *Phys. Rev. C* **6**, 6 (1972)
[61] P Schwandt, Ronald E Brown, F D Correll, R A Hardekopf and G G Ohlsen, *Phys. Rev. C* **26**, 369 (1982)
[62] J Lubian *et al*, *Nucl. Phys. A* **791**, 24 (2007)
[63] A A Rudchik *et al*, *Phys. Rev. C* **72**, 034608 (2005)